Molecular Crystals and Liquid Crystals Science and Technology. Section A. Molecular Crystals and Liquid Crystals

Publication details, including instructions for authors and subscription information:
http://www.tandfonline.com/loi/gmcl19

Effect of Organic Cation A on the Crystal Structure and Magnetisation of the Layer Molecular Ferrimagnets $AFe^{II}Fe^{III}(C_2O_4)_3$

Christopher J. Nuttall [a] , Simon G. Carling [a] & Peter Day [a]

[a] Davy Faraday Research Laboratory, The Royal Institution of Great Britain, 21 Albemarle Street, London, W1X4BS, UK

Version of record first published: 24 Sep 2006

To cite this article: Christopher J. Nuttall, Simon G. Carling & Peter Day (1999): Effect of Organic Cation A on the Crystal Structure and Magnetisation of the Layer Molecular Ferrimagnets $AFe^{II}Fe^{III}(C_2O_4)_3$, Molecular Crystals and Liquid Crystals Science and Technology. Section A. Molecular Crystals and Liquid Crystals, 334:1, 615-630

To link to this article: http://dx.doi.org/10.1080/10587259908023356

Mol. Cryst. and Liq. Cryst., 1999, Vol. 334, pp. 615-630
Reprints available directly from the publisher
Photocopying permitted by license only

Effect of Organic Cation A on the Crystal Structure and Magnetisation of the Layer Molecular Ferrimagnets $AFe^{II}Fe^{III}(C_2O_4)_3$

CHRISTOPHER J. NUTTALL, SIMON G. CARLING and PETER DAY

Davy Faraday Research Laboratory, The Royal Institution of Great Britain, 21 Albemarle Street, London W1X 4BS, UK.

We survey the crystal and magnetic structures and bulk magnetisation for representative examples of the series of ferrimagnetic tris-oxalato-ferrate(II,III) salts with general formula $AFe^{II}Fe^{III}(C_2O_4)_3$ (A = quaternary ammonium, phosphonium). The compounds all crystallise in two-dimensional hexagonal honeycomb lattices but while some show positive magnetisation at low temperature (Néel type Q) others show a large negative magnetisation below a compensation temperature T_{comp} (Néel type N). In compounds that exhibit negative magnetisation a discontinuity in the magnetisation is observed at T_t ($T_{comp} < T_t < T_c$) indicative of a magneto-strictive transition. In compounds that exhibit positive magnetisation, hysteresis and frequency dependent AC susceptibility indicate a glassy magnetic order at low temperatures, possibly arising from the frustration of random anisotropy domains below a blocking temperature, or imbalance and disorder of Fe(II) and Fe(III).

INTRODUCTION

One of the most remarkable features of molecular-based materials is the way that the magnetic properties may be transformed by quite small and subtle variations in the molecular chemistry[1]. A striking example of this general statement is the elegant and diverse series of two-dimensional molecular-based magnetic materials formed by tris-oxalato-salts containing both divalent and trivalent transition metal ions and a wide range of organic cations, principally tetra-alkyl and tetra-aryl-phosphonium, arsonium and ammonium[2]. The common formula is $AM^{II}M'^{III}(C_2O_4)_3$ (A = organic cation) and the M and M' alternate in a hexagonal planar honeycomb lattice, bridged by the ambidentate oxalate ions[3-5]. We surveyed the structures and magnetic properties of a large number of $Mn^{II}Fe^{III}$ and $Fe^{II}Fe^{III}$ examples with different A and found that the magnetic ground state was extremely sensitive to small chemical variations in A[6]. In particular, we found that in

the $Fe^{II}Fe^{III}$ series the low field magnetisation became large and negative at low temperature for some A, but not others[7]. Essentially, the compounds behaved as N-type or Q-type according to Néel's classification of ferrimagnets[8].

The connectivity of the honeycomb layer requires adjacent *tris*-oxalate units to have alternating enantiomeric configurations, D and L, so that, within a given layer all the M have one configuration and all the M' the other. The inorganic layers are interleaved by organic cations, A, whose size controls the interlayer separation[6]. A large number of compounds with this general formula have been reported by varying M, M' and A[3,6,9,10], and consequently a wide variety of magnetic ground states have been achieved; including ferro, antiferro and a range of ferrimagnets[13], though crystal structures from single crystal X-ray diffraction are available only for a limited number of examples owing to the difficulty in obtaining suitable crystals [3-5,11]. Nevertheless, it is clear that the layer honeycomb topology is maintained throughout the series, while the organic cation plays an important part in determining the stacking of the layers, as well as the precise local symmetry at the metal ion sites. This point is illustrated by the layer stacking sequences found within the homologous series $N(n\text{-}C_nH_{2n+1})_4M^{II}M^{III}(C_2O_4)_3$ (n = 3 - 5) for which full structures are available (Table 1). In orthorhombic $N(n\text{-}C_5H_{11})_4\ Mn^{II}Fe^{III}(C_2O_4)_3$ the inorganic layers stack in a two layer [a-b'] repeat structure[5] (where ' indicates a reversal of metal *tris*-oxalate configurations within layers). The arrangement of the metal ions in this structure is illustrated in Figure 1. Among $N(n\text{-}C_4H_9)_4M'^{II}M^{III}(C_2O_4)_3$ compounds, two hexagonal structural refinements have been reported: that of $N(n\text{-}C_4H_9)_4Mn^{II}Cr^{III}(C_2O_4)_3$ refined in $R3c$[4], and $N(n\text{-}C_4H_9)_4Mn^{II}Fe^{III}(C_2O_4)_3$ refined in $P6(3)$[11]. The stacking of inorganic layers in the two structures is illustrated in Figure 2. The $R3c$ structure has a six-layer [a-b'-c-a'-b-c'] repeat, whilst that in $P6(3)$ is [a-b]. Finally, $N(n\text{-}C_3H_7)_4Mn^{II}Cr^{III}(C_2O_4)_3$ has also been refined in $R3c$ with the same stacking sequence[11] as that of $N(n\text{-}C_4H_9)_4Mn^{II}Cr^{III}(C_2O_4)_3$.

(cation)	$M^{II}M'^{III}$	T (K)	Space Group	Unit cell (Å)	V. (Å^3)	Ref.
$N(n\text{-}C_3H_7)_4$	MnCr	RT	$R3c$	$a = 9.363,\ c = 49.207$	3736	8
$N(n\text{-}C_4H_9)_4$	MnCr	RT	$R3c$	$a = 9.414,\ c = 53.66$	4118	6
$N(n\text{-}C_4H_9)_4$	MnFe	RT	$P6(3)$	$a = 9.482,\ c = 17.827$	1388	8
$N(n\text{-}C_5H_{11})_4$	MnFe	120	$C222(1)$	$a = 9.707,\ b = 16.140,\ c = 19.883$	3115	7

TABLE 1: Space groups and unit cell constants of $N(n\text{-}C_nH_{2n+1})_4MM'(C_2O_4)_3$ determined by single crystal X-ray diffraction.

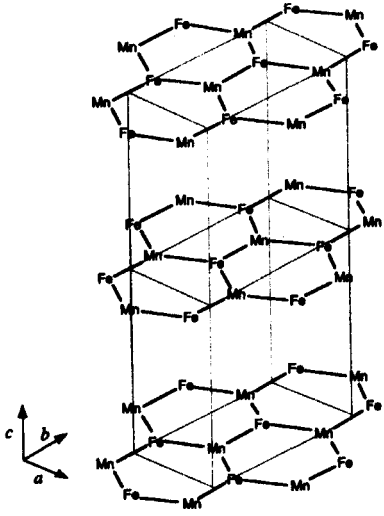

FIGURE 1: The inorganic layer framework in N(n-C_5H_{11})$_4$MnFe(C_2O_4)$_3$.

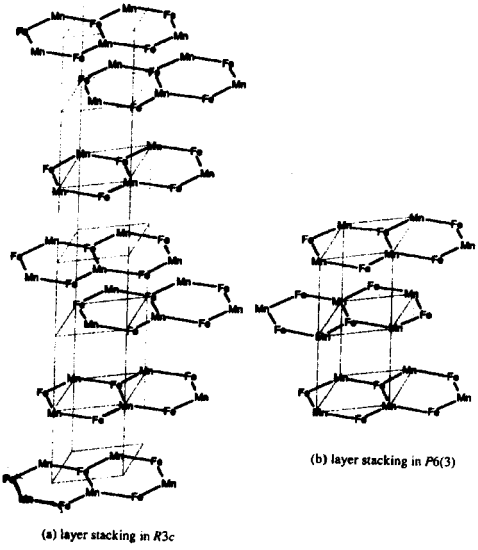

FIGURE 2: The inorganic layer framework in the (cation)MM'(C_2O_4)$_3$ structures: (a) $R3c$, (b) $P6(3)$.

The unusual magnetic properties of the series $AM^{II}Fe^{III}(C_2O_4)_3$ {M^{II} = Mn, Fe} whose low temperature magnetisation varies greatly with the organic cation A, have been studied using polycrystalline samples[6]. Powder X-ray diffraction profiles of these materials show a variety of unusual effects such as peak broadening, large peak asymmetry at low angle and sharp decreases in reflection intensities at high scattering angles, indicative of structural disorder. The degree of disorder also depends on the details of the synthetic route.

Measuring the time dependence of the angular asymmetry in the decay of spin polarised muons implanted in a magnetic sample has been shown to provide sensitive information about the local magnetic environment, because the muon spin precesses around any internal field generated in its neighbourhood. Muon spin rotation has also been measured in two compounds from the $AFe(II)Fe(III)(C_2O_4)_3$ series, chosen to represent respectively type N (A = $N(n\text{-}C_4H_9)_4$) and type Q (A = $P(C_6H_5)_4$) behaviour[21].

Finally, definitive evidence on the ordered magnetic structures of solids comes from neutron diffraction. The only published work on the magnetic structure of a layer bimetallic tris-oxalate salt using this method referred to a Mn(II)Cr(III) phase which is ferromagnetic[12]. Here we survey results from a neutron powder diffraction study of the two antiferromagnetic phases $P(C_6D_5)_4M^{II}Fe(C_2O_4)_3$ with M^{II} = Mn and Fe.

Crystal and Magnetic Structure

In layered materials structural disorder frequently arises from poor correlation between the orientation of adjacent layers arising from translation of the rigid planes. Two limiting cases of disorder may be identified. In one case layers stack in a random fashion with a complete loss of inter-planar registry. The coherent diffraction intensity is only observed for [00l] reflections, [hk0] reflections exhibiting weak two-dimensional diffraction and [hkl] reflections having no coherent scattering intensity[13]. In the second case, there is a finite number of possible translational vectors between successive layers. This type of layer disorder, known as stacking faulting, results in streaks in the reciprocal lattice, giving [hkl] dependent broadening of peaks in the powder diffraction pattern[14]. We simulated X-ray powder diffraction patterns of the $N(n\text{-}C_3H_7)_4$ compounds with both $R3c$ and $P6(3)$ layer stacking and also for cases where the stacking is faulted between each type[14,15]. The crystal is defined by infinite sheets of layer unit cells stacked in sequence with defined stacking vectors ($\boldsymbol{R}_{ij}$) between adjacent layers. Faulting is simulated by introducing alternative layers and/or stacking vectors within a layer sequence by using stacking probabilities (a_{ij}) for each possible $\boldsymbol{R}_{ij}$.

The X-ray powder diffraction profiles of the $N(n\text{-}C_4H_9)_4$ and $N(n\text{-}C_3H_7)_4$ compounds have previously been indexed by relaxing the $R3c$ reflection conditions[6]. Fitting the structural models now available from

single crystal X-ray diffraction to the powder profiles reveals that precipitated polycrystalline samples are in fact biphasic, containing contributions from both *P*6(3) and *R*3*c* phases. The reflections attributed to the *P*6(3) phase are broader and their line shapes have larger Lorentzian contributions compared to those from the *R*3*c* phase. Given the similarity of layer stacking in the *R*3*c* and *P*6(3) structures, there is a strong possibility that each powder-crystallite contains both stacking types, i.e. the compounds suffer from stacking faults. Powder diffraction profiles of the faulted layer structure were then calculated for different faulting probabilities, n (Figure 3(a)), while the measured profile of $N(n\text{-}C_3H_7)_4MnFe(C_2O_4)_3$ is displayed for comparison in Figure 3(b).

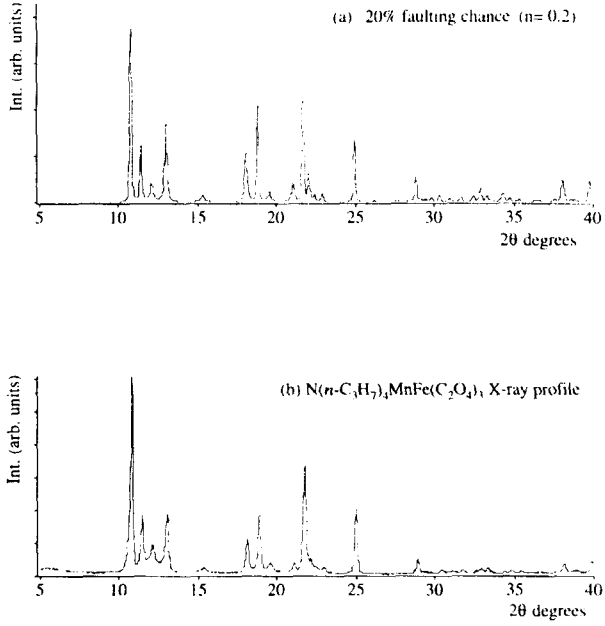

FIGURE 3: X-ray powder diffraction profiles of $N(n\text{-}C_3H_7)_4MnFe(C_2O_4)_3$ (a) calculated for a 20% faulting probability; (b) measured.

A faulting chance of 1% between *P*6(3) and *R*3*c* gives a calculated X-ray profile equivalent to the sum of *R*3*c* and *P*6(3) phases, since it corresponds to ~100 *R*3*c* or *P*6(3) cells between faults. Faulting probabilities (above 20% result in an overall broadening of the reflections. Reflections originating from the *P*6(3) phase become relatively weaker with increasing faulting probability and their lineshapes exhibit large Lorentzian broadening. The same effect is also noticable in the N(*n*-

$C_3H_7)_4MnFe(C_2O_4)_3$ experimental profile. The closest correspondance between observed and simulated profiles corresponds to a faulting probability of between 20 and 30%.

The neutron powder diffraction profile of the MnFe compound is displayed in Figure 4(a), and that of the FeFe compound is in Figure 2(b). Using profile matching[16], i.e. iterative fitting of structure factors, both were fitted with a Gaussian peak shape and *R*3*c* unit cell. The intensity not fitted by the profile matching procedure is attributed to one small fraction of *P*6(3) stacking phase identified in X-ray diffraction profiles. In the MnFe compound a number of reflections had increased intensity at 1.5K due to magnetic diffraction arising from long range magnetic order. In contrast, in the FeFe compound the only extra intensity at 1.5K is a weak shoulder to the [202] nuclear reflection.

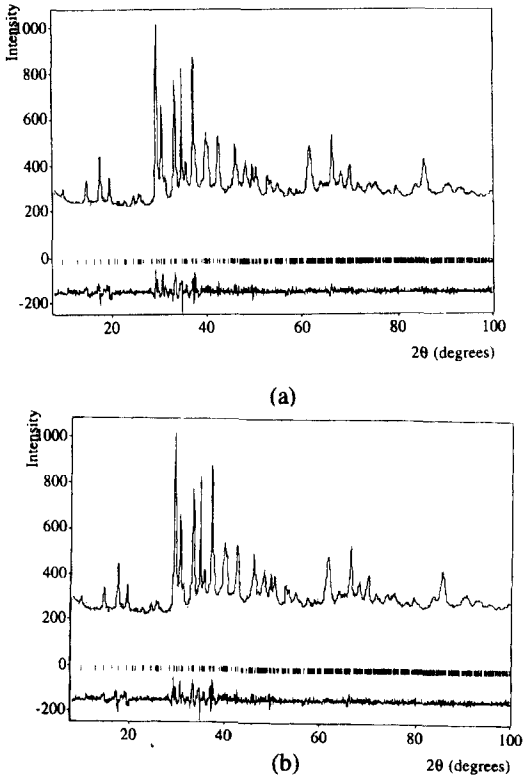

FIGURE 4: Neutron diffraction profiles of $P(C_6D_5)_4M^{II}Fe(C_2O_4)_3$ fitted with pattern matching to an *R*3*c* cell: (a) M^{II} = Mn, 40K; (b) M^{II} = Fe, 50K

The magnetic diffraction intensity was investigated in greater detail by means of difference plots. The magnetic reflections are quite weak but this can be indexed using a *R*3*c* cell. The indices of the magnetic reflections of MnFe (Figure 5(a)) indicate that the chemical and magnetic cells are coincident, i.e. the magnetic structure has the propagation vector $\boldsymbol{k} = 0$, and also that the moments lie close to the *c*-axis, since no intensity is found for [00l] reflections. Two models are generated: respectively these are *R*3*c* and *R*3*c*' according to the Shubnikov definition. They differ in that *R*3*c* requires the orientations of Mn and Fe moments to alternate from up to down in adjacent layers while in *R*3*c*' they have the same relative orientation in all layers. Comparing the observed and predicted patterns it is clear that the *R*3*c* Shubnikov group provides the best representation of the low temperature magnetic order in the Mn, Fe compound. The proposed magnetic structure is illustrated in Figure 6. There are a few reflections in the magnetic profile which are not predicted by this model. The extra magnetic intensity could result from either the presence of a small amount of a *P*6(3) stacking phase previously identified or from magnetic order in *R*3*c* with moments not exactly aligned along the *c*-axis.

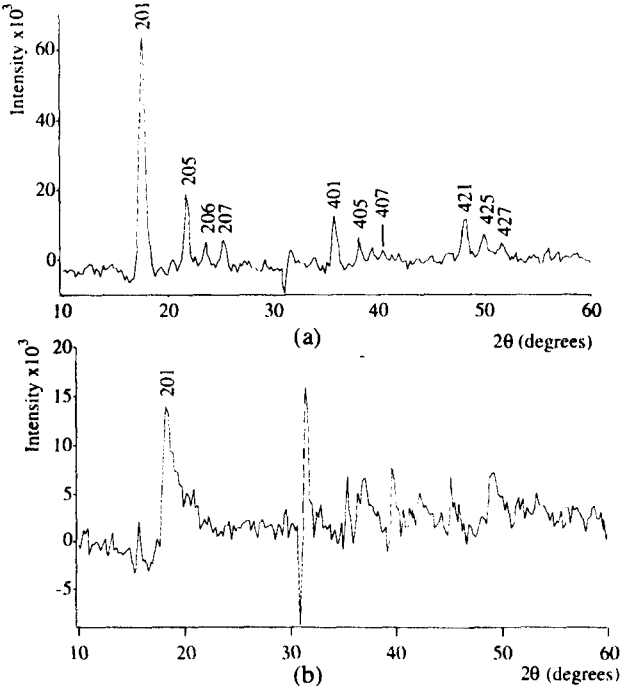

FIGURE 5: Intensity difference [I(1.7K) - $I(T>T_c)$] for $P(C_6D_5)_4M^{II}Fe(C_2O_4)_3$ with magnetic reflections (*R*3*c* cell) indicated: (a) M^{II} = Mn, T = 30K; (b) M^{II} = Fe, T = 50K

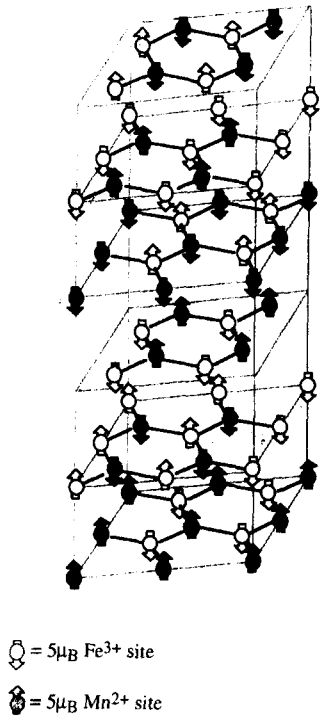

FIGURE 6: Proposed magnetic structure of $P(C_6D_5)_4MnFe(C_2O_4)_3$

In contrast to the MnFe compound, the intensity difference plot [I(1.7K) - I(50K)] of the FeFe compound (Figure 5(b)), reveals only extremely weak magnetic scattering. That the single clearly observed peak indexes as [201] indicates antiferromagnetic order of the Fe(II) and Fe(III) moments parallel to the *c*-axis. However, the [201] reflection is highly asymmetric, which strongly suggests that there is disorder between the layers. Nevertheless, the bulk susceptibility measurements suggested a transition to long-range order at 34K[6]. In view of these facts, one possible view of the magnetic order is that the behaviour is glassy as a result of the strong single ion anisotropy of the Fe(II) ions: below 39K ferrimagnetic correlations develop with anisotropy directions randomly oriented in different layers. Finally the correlated regions become blocked by each other so that, while the majority of the moments are fixed by anisotropy pinning, a fraction remains mobile down to 5K. This conclusion is confirmed by the bulk magnetisation measurements described below.

Figure 7 shows the temperature dependence of the initial asymmetries (a_0) in the decay of spin polarised muons for the $N(n\text{-}C_4H_9)_4$ and $P(C_6H_5)_4$ $Fe^{II}Fe^{III}$ compounds. The sharp drop in a_0 occurs at the magnetic ordering transition, i.e. around 43K for the $N(n\text{-}C_4H_9)_4$ compound and 37K for the $P(C_6H_5)_4$ one, (T_c = 43.5K and 34K, respectively from the bulk susceptibility). The fall in a_0, which is steeper in $N(n\text{-}C_4H_9)_4FeFe(C_2O_4)_3$ than $P(C_6H_5)_4FeFe(C_2O_4)_3$ indicates that muon relaxation or resonance processes are faster than the spectrometer can measure.

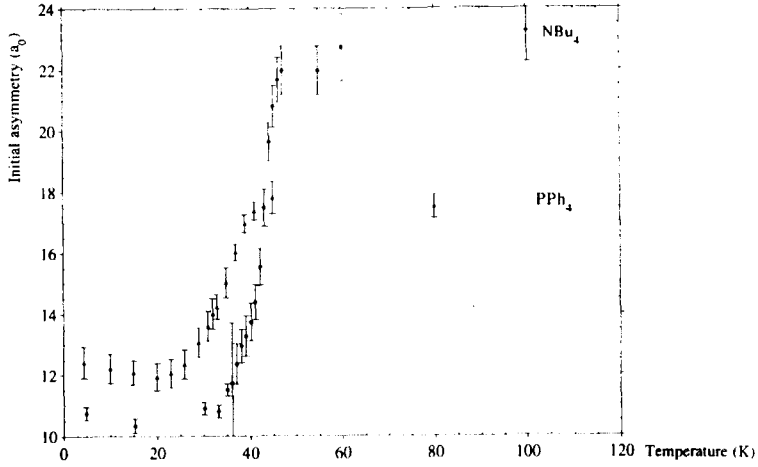

FIGURE 7: The temperature dependence of initial asymmetries of muon spin rotation in $AFeFe(C_2O_4)_3$ ($A=N(n\text{-}C_4H_9)_4$; $P(C_6H_5)_4$).

In magnetic insulators with a high moment, losses in muon asymmetry normally occur with the onset of magnetic order, and the proportion of the initial asymmetry lost measures the degree of magnetic order in the sample. In a fully ordered magnet one third of static moments in a powder sample are aligned parallel to the initial muon polarisation in a sample with randomly orientated microcrystallites. The muons that experience static fields parallel to their spin direction retain their polarisation and contribute a non-oscillating component, so we expect a_0 to fall to 33% of the high temperature asymmetry at the transition to long-range magnetic order. In $N(n\text{-}C_4H_9)_4FeFe(C_2O_4)_3$ $a_0(4.5K)/a_0(100K)$ is 46%, whilst in $P(C_6H_5)_4FeFe(C_2O_4)_3$ $a_0(4.5K)/a_0(80K)$ is about 70%, suggesting that long-range order is established more fully throughout the sample in the former than the latter.

Magnetic Susceptibility and Magnetisation

Before looking at the unusual magnetic properties of the $AFe^{II}Fe^{III}(C_2O_4)_3$ compounds in their ordered state we first consider their behaviour in the

paramagnetic region. The susceptibilities of all members of the series obey the Curie-Weiss law from 150 to 300K. The mean value of the Curie constant across the series ($7.662 cm^3 mol^{-1} K$) is consistent with the presence of high spin Fe^{III} and Fe^{II} ions: assuming spin-only moments $S(Fe^{III}) = 5/2$ and $S(Fe^{II}) = 2$ and an isotropic Landée splitting factor, g= 2, for both ions calculates $C = 7.375 cm^3 mol^{-1} K$.

Whilst it is a good approximation to the $^6A_{1g}$ ground state of the Fe^{III} ion, the assumption of a spin-only moment is a poor approximation for Fe^{II}. The ^5D (L = 2) free-ion state of $Fe^{II}(d^6)$ ions has orbital degeneracy and in a cubic ligand field the $^5T_{2g}$ ground term retains an orbital contribution to the total moment, so that the lowest spin orbit state has J = 1. Introducing a trigonal distortion from the three bidentate oxalate ligands causes a further splitting of the J = 1 state so that the resulting ground state is either a singlet ($M_J = 0$) or doublet ($M_J = +/-1$)[17]. The energy separation between the spin-orbit components in Fe^{II} is the order of $200 cm^{-1}$ so we expect an orbital contribution to the Fe^{II} moment, which could explain the high value of the Curie constant. The Curie constants of $N(n\text{-}C_3H_7)_4$, $N(n\text{-}C_4H_9)_4$ and $P(n\text{-}C_4H_9)_4$ compounds are all in excess of the spin-only value by approximately $0.43 cm^3 Gmol^{-1}$; however, for $N(n\text{-}C_5H_{11})_4Fe^{II}Fe^{III}(C_2O_4)_3$ C = $9.05 cm^3 Gmol^{-1}$ (Table 1). This correlates with the different symmetry of the Fe^{II} sites: for $N(n\text{-}C_3H_7)_4$, $N(n\text{-}C_4H_9)_4$ and $P(n\text{-}C_4H_9)_4$ compounds the powder X-ray diffraction fits a hexagonal cell with C_3 site symmetry of the $Fe^{II}(C_2O_4)_3$ unit[6], while the site symmetry of Fe^{II} in the $N(n\text{-}C_5H_{11})_4$ compound is C_2[6]. The Weiss constants q are all large and negative (Table 1). The magnetic exchange is of similar strength in all the compounds, as expected, given the close similarity between the structures. In most of the compounds $|T_c/q| \approx 0.5$ although for $P(C_6H_5)_4$ and $As(C_6H_5)_4$ it is ≈ 0.4. Molecular field theory predicts $|T_c/q| = 1$, but large deviations are expected in low dimensional magnets because of the build up of short-range correlations above T_c. Indeed, for a two-dimensional Ising ferromagnet on a honeycomb lattice $|T_c/q|$ has been calculated as 0.506[18]. The reduced $|T_c/q|$ in the $P(C_6H_5)_4$ and $As(C_6H_5)_4$ compounds, may therefore signal a change in the effective dimensionality.

Below 100K the magnetisation of this series of compounds varies dramatically with the cation A. When measuring the magnetisation after cooling in a 100G field, a magnetic compensation point (T_{comp}) and low temperature negative magnetisation with respect to the field, is observed in the A = $N(n\text{-}C_3H_7)_4$, $N(n\text{-}C_4H_9)_4$, $N(n\text{-}C_5H_{11})_4$, $P(n\text{-}C_4H_9)_4$ and PPN compounds whilst the $P(C_6H_5)_4$ and $As(C_6H_5)_4$ compounds show a positive magnetisation at low temperature. Since all the compounds are ferrimagnetic, the temperature dependence of the magnetisation can be compared with that predicted by Néel: the 'normal' positive magnetisation curves of the $P(C_6H_5)_4$ and $As(C_6H_5)_4$ compounds resemble the Néel type

Q ferrimagnetic order whilst the negative magnetisation curves exhibit a variant of Néel type N order. According to Néel, the ground state of a ferrimagnet is determined by the saturation magnetisations of each magnetic sublattice ($M_s(T = 0K)$) and their relative ordering rates with respect to temperature. A compensation temperature (T_{comp}) should occur in the magnetisation if the sublattice with the smaller saturation magnetisation initially orders more rapidly with decreasing temperature than the one with the larger saturation magnetisation. In the honeycomb lattice with alternating Fe^{II} and Fe^{III} ions, this situation corresponds to an initially steeper ordering on the Fe^{II} sublattice.

Evidence concerning the sublattice ordering in the $Fe^{II}Fe^{III}$ compounds comes from the Mössbauer spectra of the $N(n\text{-}C_4H_9)_4$ and $P(C_6H_5)_4$ compounds, from which the hyperfine field at the Fe^{III} nucleus has been extracted as a function of temperature for both compounds[19]. Within the molecular field approximation, the field experienced at the Fe^{III} nucleus is the sum of exchange fields which, to a first approximation, originate from the neighbouring Fe^{II} ions. Hence, the development of a hyperfine field at the Fe^{III} nucleus provides a measure of the magnetisation of the Fe^{II} sublattice and *vice versa*. The Mössbauer data indicate that there is a sharp increase in the Fe^{II} sublattice magnetisation in the $N(n\text{-}C_4H_9)_4$ compound below 40K, which the Fe^{II} hyperfine field was not fully developed ($H_{int} \sim 5T$ at 1.9K). This provides evidence that the Fe^{II} sublattice does indeed order at a higher temperature than Fe^{III} in the $N(n\text{-}C_4H_9)_4$ compound. The situation in the $P(C_6H_5)_4$ case is more complex, with a hyperfine splitting at the Fe^{III} nucleus occurring only below 25K.

It is not appropriate to extract molecular field parameters because the honeycomb lattice is two-dimensional and therefore deviates considerably from the molecular field approximation as can be seen by the fact that $|T_c/q| \leq 0.5$. Furthermore, the Fe^{II} ion exhibits an orbital moment and hence its magnetisation does not follow a Brillouin function. Finally, spin-orbit coupling in Fe^{II} introduces considerable anisotropy into the system that is not accounted for by the molecular field model.

Figure 8 illustrates two ways in which the magnetisation in Néel type N ferrimagnets can vary with temperature. Either the magnetic pole reverses, i.e. $\{Fe^{II}(\neq)Fe^{III}(\emptyset)$ Æ $Fe^{II}(\emptyset)Fe^{III}(\neq)\}$ at T_{comp}, resulting in positive magnetisation at low temperature or the initial magnetic pole direction is maintained and the magnetisation becomes negative below T_{comp}. $N(n\text{-}C_4H_9)_4Fe^{II}Fe^{II}(C_2O_4)_3$ behaves like the latter, although thermodynamically, positive magnetisation is favoured over negative at low temperature. In the molecular field approximation with fully isotropic exchange fields, there is no energy barrier to magnetic pole reversal, leading to positive magnetisation. The fact that the $N(n\text{-}C_4H_9)_4$ is negative indicates

that there is a barrier due to anisotropy sufficient to hinder pole reversal at T_{comp}.

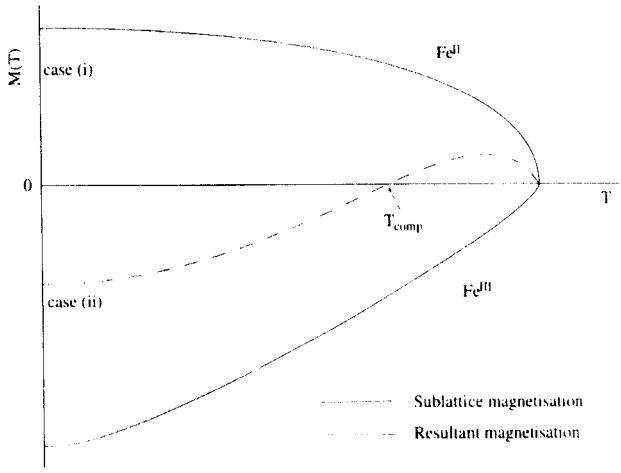

FIGURE 8: Magnetic sublattice ordering in a ferrimagnet containing Fe^{II} and Fe^{III} with Néel type N order.

Parameters describing the temperature dependent hysteresis in the $N(n\text{-}C_4H_9)_4$ compound are displayed in Figure 9, from which it is clear that the onset of giant anisotropy (H_c > 10,000G) and the magnetic memory effect both occur between 36K and 38K. Also the divergence in coercivity clearly correlates with narrowing of the hysteresis. The pronounced change in magnetic characteristics between 36K and 38K indicates that some form of magneto-strictive transition occurs between T_c and T_{comp}. Further evidence that there is such a transition comes from low field measurements. The shoulder at 40K in the ZFC magnetisation is revealed as a discontinuity in the 100G FC case, and similar discontinuities in the FC magnetisation in all members of the series with negative magnetisation at low temperature, but the field cooling history through T_t and not T_c determines the low temperature negative magnetisation: the negative magnetisation is only reversed after cooling through T_c and T_t in fields ≥ 60,000G.

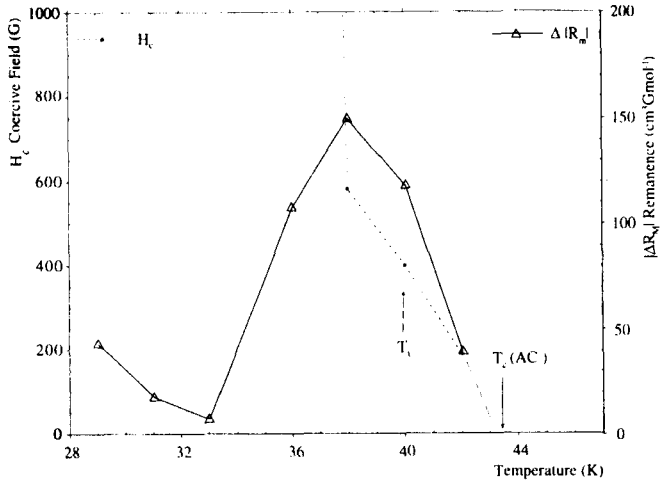

FIGURE 9: The temperature dependent hysteresis parameters of $N(n\text{-}C_4H_9)_4Fe^{II}Fe^{III}(C_2O_4)_3$.

We conclude that the first order discontinuity in the magnetisation at T_t is the factor determining the low temperature magnetisation properties of $(cation)Fe^{II}Fe^{III}(C_2O_4)_3$ compounds with negative magnetisation, though the physical origin of the transition has not been identified. One possibility is that at T_t the Fe^{II} moments lock due to an orbital ordering. If so, then cooling through T_t in small applied fields would provide the Fe^{II} moments with a preferred ordering direction. Provided the ferrimagnetic order conforms to the Néel type N, the magnetisation will then become negative at low temperatures. The anisotropy developing below T_c due to a magneto-strictive orbital ordering of the Fe^{II} moments would be very large, as observed. A structural phase transition should also occur at T_t as the Fe^{II} moments couple to the lattice, but to date there are no low temperature structural data on any of these compounds. Nevertheless, the discontinuity in the magnetisation points strongly to such a phase transition.

Returning to the magnetisation behaviour in $P(C_6H_5)_4$ and $As(C_6H_5)_4$ compounds, which correspond to Néel type Q ferrimagnetic order, one question remaining is why there is such a large difference between the magnetic behaviour in these compounds and those behaving like Néel type N. First, the transition to long-range magnetic order is less abrupt, and the AC susceptibility shows no sharp peak, either in dispersion or absorption. It is also strongly frequency dependent, while hysteresis is only observed below 25K. The temperature dependence of the hysteresis parameters of the $P(C_6H_5)_4$ salt (Figure 10) are quite different from those of the $N(n\text{-}C_4H_9)_4$ one (Figure 9).

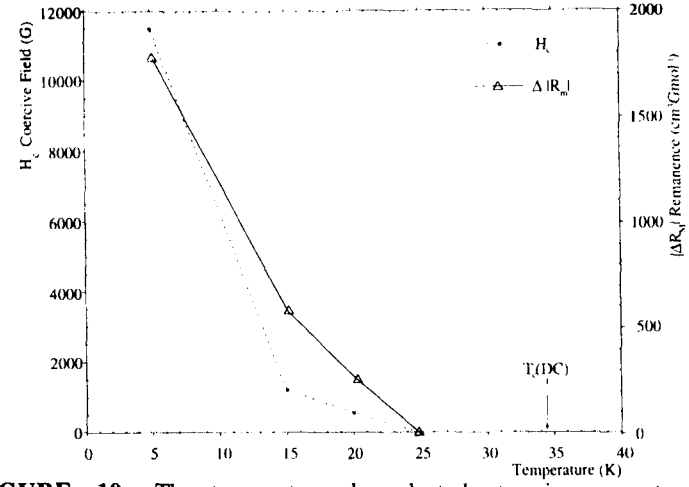

FIGURE 10: The temperature dependent hysteresis parameters of $P(C_6H_5)_4Fe^{II}Fe^{III}(C_2O_4)_3$.

Neutron powder diffraction of $P(C_6D_5)_4Fe^{II}Fe^{III}(C_2O_4)_3$ reveals only weak asymmetric magnetic scattering intensity below 38K at the [201] reciprocal lattice point, attributed to moments ordering parallel to the *c*-axis[120]. Thus weak scattering indicates that long-range magnetic order is not completely developed, even at 5K, either as a result of a finite spin correlation length or because only part of the sample undergoes a transition to long-range magnetic order. All these strands of evidence point to the magnetic order in $P(C_6H_5)_4Fe^{II}Fe^{III}(C_2O_4)_3$ as being glassy. Below 34K ferrimagnetic correlations begin to develop with randomly oriented anisotropy, so that at 22-25K the correlated regions become blocked by one another and hysteresis develops. Below the blocking temperature the bulk of the moments are fixed by anisotropy pinning, whilst a fraction remains mobile down to 5K. The reasons for such glassy magnetic ordering could lie in a small deficiency of Fe and the charge compensating oxidation process $Fe^{II}ÆFe^{III}$ which introduces disorder in the magnetic sublattices.

CONCLUSIONS

Our aim has been to map and then identify the reason for the appearance of negative magnetisation at low temperature in $N(n\text{-}C_4H_9)_4$ Fe^{II} Fe^{III} $(C_2O_4)_3$ but not in the $P(C_6H_5)_4$ salt. The two types of behaviour correspond to Néel's type N and Q categories of ferrimagnetism. The negative magnetisation becomes established above very low cooling fields (2G) and increases in magnitude until around 2,000G. After field cooling,

the magnetisation remanence at 5K displays an asymmetric hysteresis with a giant anisotropy. The onset of giant anisotropy correlates with a discontinuity in the magnetisation at $T_t = 40K$ ($T_{comp} < T_t < T_c$) assigned to a magneto-strictive transition, accompanied by alignment of the Fe^{II} local anisotropy axes. It is this transition that is responsible for the stability of the negative magnetisation. By contrast, in the $P(C_6H_5)_4$ compound, where no such discontinuity is found, full long-range magnetic order is not achieved, but a proportion of the moments remain mobile well below T_c. More detailed crystallographic studies at low temperature will be needed to answer the final key question as to why the substitution of one organic cation by another should trigger such a profound change in the magnetic order in these otherwise very similar lattices.

ACKNOWLEDGEMENTS

Our group has been supported by the UK Engineering and Physical Sciences Research Council and the European Commission TMR Programme.

References

[1] For numerous recent examples, see e.g. Kahn, O. (ed.) *Magnetism a Supramolecular Function;* Dordrecht, Kluwer Academic Publishers, **1996.**

[2] Tamaki, H.; Zhong, Z.J.; Matsumoto, N.; Kida, S.; Koikawa, M.; Achiwa, N.; Hashimoto, Y.; Ookawa, H. *J. Am. Chem. Soc.* **1992,** *114,*6974–6979.

[3] Decurtins, S.; Schmalle, H.W.; Oswald, H.R.; Linden, A.; Ensling, J.; Gutlich, P.; Hauser, A. *Inorganica Chimica Acta* **1994,**65–73.

[4] Atovymann, O.L.; Shilov, G.V.; lyubovskaya, R.N.; Zhilyaeva, E.I.; Ovaneseyan, N.S.; L., P.S.; Gusakovskaya, I.G.; G., M.Y. *JETP Letters* **1993,** 58, 767–768.

[5] Carling, S.G.; Mathonière, C.; Day, P.; Malik, K.M.A.; Coles, S. J.; Hursthouse, M.B., *J. Chem. Soc. Dalton Trans.* **1996,** 1839.

[6] Mathoniere, C. ; Nuttall, C.J.; Carling, S.G. ; Day, P. *Inorganic Chemistry* **1996,** *35,* 1201–1207.

[7] Mathoniere, C.C., S.G.; Yusheng, D.; Day, P. *J. Chem. Soc. Chemical Commun.* **1994,** 1551–1552.

[8] Neel, L. *Annales de Phys.* (Paris) **1948,** 3, 137–198.

[9] H. Tamaki, M. Mitsumi, K. Nakamura, N. Matsumoto, S. Kida, H. Ookawa, S. Iijima, *Chem. Lett.,* **1992,** 1975.

[10] Clemante-Leon, M.; Coronado, E.; Galan-Mascaros, J.R.; Gomez-Garcia, J., *J.C.S. Chem. Commun.,* 1997, 1727.

[11] Decurtins, S.; Schmalle, H.W.; Pellaux, R.; Schneuwly, P.; Hauser, A., *Inorg. Chem.* **1996,** *35,* 1451.

[12] Pellaux, R.; Schmalle, H.W.; Huber, R.; Fischer, P.; Hauss, T.; Ouladdiaf, B.; Decurtins, *S. Inorg. Chem.* **1997,** *36,* 2301.

[13] Warren, B.E., *Phys. Rev.* **1941,** *59,* 693.

[14] Treacy, M.M.J.; Newsham, J.M.; Deem, M.W., *Proc. Roy. Soc. London (A)* **1991,** *433,* 499.

[15] Treacy, M.M.J., "DIFFaX v1.766 (The Manual)", **1991.**

[16] Rodriguez-Carvajal, J. *FULLPROF. Reference Guide to the Program 3.2,* Paris, CEA-CNRS, **1997.**

[17] Figgis, B. N. *Introduction to Ligand Fields;* Interscience Publishers John Wiley and Sons:, **1961.**
[18] De Jongh, L. J. *Magnetic Properties of Layered Transition Metal Compounds;* Kluwer Academic Press:, **1990;** Vol. 9.
[19] Ensling, J. ; Nuttall, C. J.; Day, P. to be published.
[20] Nuttall, C.J.; Day, P., *Inorg. Chem.*, **1998,** 37, 3885.
[21] Nuttall, C.J.; Carling, S.G.; Day, P., to be published.
[22] Nuttall, C.J. and Day, P., *Chem. Mater.*, **1998,** 10, 3050.